



Predictive modeling of haloacetonitriles under uniform formation conditions

Gamze Ersan ^a, Mahmut S. Ersan ^b, Amer Kanan ^c, Tanju Karanfil ^{a,*}

^a Department of Environmental Engineering and Earth Sciences, Clemson University, Anderson, SC, 29625, United States

^b School of Sustainable Engineering and The Built Environment, Arizona State University, Tempe, AZ, 85287-5306, United States

^c Department of Environment and Earth Sciences, Faculty of Science and Technology, Al-Quds University, Palestine

ARTICLE INFO

Keywords:

Haloacetonitriles
Predictive modeling
Uniform formation conditions
Chlorination
Chloramination
Prechlorination

ABSTRACT

The objective of this study was to develop models to predict the formation of HANs under uniform formation conditions (UFC) in chlorinated, choraminated, and perchlorinated/chloraminated waters of different origins. Model equations were developed using multiple linear regression analysis to predict the formation of dichloroacetonitrile (DCAN), HAN4 (trichloroacetonitrile [TCAN]), DCAN, bromochloroacetonitrile [BCAN], and dibromoacetonitrile [DBAN]) and HAN6 (HAN4 plus monochloroacetonitrile, monobromoacetonitrile). The independent variables covered a wide range of values, and included ultraviolet absorbance (UV₂₅₄) dissolved organic carbon (DOC), dissolved organic nitrogen (DON), specific UV absorbance at 254 (SUVA₂₅₄), bromide (Br⁻), pH, oxidant dose, contact time, and temperature. The regression coefficients (r^2) of HAN4 and HAN6 models for natural organic matter (NOM), algal organic matter (AOM), and effluent organic matter (EfOM) impacted waters were within the range of 60–88%, while the r^2 values of HAN4 and DCAN models for both groundwater and distribution systems were lower, in the range of 41–66%. The r^2 values for the DCAN model were mostly higher in the individual types as compared to the cumulative analysis of all source water data together. This was attributed to differences in HAN precursor characteristics. For chlorination, among all variables, pH was found to be the most significant descriptor in the model equations describing the formation of DCAN, HAN4, and HAN6, and it was negatively correlated with HAN formation in the distribution system, groundwater, AOM, and NOM samples, while it showed an inverse relationship with HAN6 formation in EfOM impacted waters. During chloramination, pH was the most influential model descriptor for DCAN formation in the NOM. Prechlorination dose was the most predominant parameter for prechlorination/chloramination, and it was positively correlated with HAN4 formation in AOM impacted waters.

1. Introduction

One unintended consequence of water disinfection is the formation of halogenated disinfection byproducts (DBPs) as a result of reactions between oxidants and organic (i.e., natural organic matter [NOM], algal organic matter [AOM], and effluent organic matter [EfOM]), and inorganic (i.e., bromide [Br⁻] and iodide [I⁻]) precursors (Rook, 1974; Trehy and Bieber, 1981; Oliver, 1983; Ersan et al., 2019a; Liu et al., 2019). Although the regulated carbonaceous DBPs (C-DBPs), trihalomethanes (THMs), and haloacetic acids (HAAs), are commonly reported in distribution systems and they are of concern due to their health impacts and regulatory considerations, unregulated nitrogenous haloacetonitriles (HANs) have also been detected following chlorination or

chloramination (Bougeard et al., 2010; Krasner et al., 2006; Krasner et al., 2008; Obolensky et al., 2007; Sfynia et al., 2017). The measured molar concentration of HANs is usually one order of magnitude lower than the regulated THMs and HAAs; nevertheless, toxicology studies have shown that HANs pose up to three orders of magnitude higher cytotoxicity and genotoxicity than C-DBPs (Muellner et al., 2007; Plewa et al., 2008). Four HAN species (HAN4: dichloroacetonitrile (DCAN), trichloroacetonitrile (TCAN), bromochloroacetonitrile (BCAN), and dibromoacetonitrile (DBAN)), are the most commonly detected species in the treated waters (Krasner et al., 1989a,b). Among them, DCAN has been the most prevalent HAN species, which has been detected in the distribution system up to 9 µg/L following chlorination (Obolensky et al., 2007; Yang et al., 2008; Chen and Westerhoff, 2010). Several

* Corresponding author.

E-mail address: tkaranf@clemson.edu (T. Karanfil).

parameters including UV absorbance (UV_{254}), specific UV absorbance at 254 ($SUVA_{254}$), dissolved organic matter (DOC), dissolved organic nitrogen (DON), Br^- , pH, oxidant type and dose, reaction time, and temperature can play a role in the formation of HANs (Ersan et al., 2019a, 2019b; Liu et al., 2018).

The ability to predict the DBP formation is valuable to water utilities as solely relying on chemical analyses can be expensive and time-consuming. Several researchers have proposed different empirical models for DBP formation, as seen in Table S1 (in the Supporting Information [SI] Section). Most of these models were derived from linear and non-linear regression analysis. Compared to multiple linear regression (MLR) analysis, the nonlinear approach (i.e., especially using modern learning algorithms) is more accurate for the prediction of DBP formation, when a wide range of datasets is available (Milot et al., 2002; Platikanov et al., 2012; Ike et al., 2020), whereas the linear regression analysis is more appropriate for the much narrower DBP datasets (Ike et al., 2020). In previous studies, MLR models have been developed to predict the formation of DBPs under different range of environmental and water treatment conditions (Bergier et al., 2017; Engerholm and Amy, 2017; Feungpean et al., 2015; Chowdhury et al., 2009, 2010; Uyak et al., 2005; Sohn et al., 2004; Westerhoff et al., 2000; Morrow and Minear, 1987). In addition to their prediction capabilities, these models can also provide insights into the factors affecting DBP formation. To date, numerous models have been developed for predicting C-DBP formation in water (Table S1 in the SI section), whereas limited number of modeling studies, under formation potential (FP) test conditions or the samples were collected and analyzed from distribution systems, are available (Table 1) to predict DCAN and HAN4 formation in the presence of free chlorine (Bergier et al., 2017; Chen and Westerhoff, 2010; Chhipi-Shrestha et al., 2018; Guilherme and Rodriguez, 2017; Kolla, 2004; Mian et al., 2020) and chloramine (Lin et al., 2018). FP test employs high concentrations of oxidants to assess the precursor levels of DBPs in water. We recently showed that measuring HANs under FP conditions has limitations because of the decomposition of HANs at elevated free chlorine concentrations. This may cause an underestimation of HAN precursors in water (Kanan and Karanfil, 2020). There is currently no HAN model in the literature under the uniform formation conditions (UFC), a test method developed for the representative conditions of distribution systems in the United States (Summers et al.,

1996).

To the best of our knowledge, this study is the first comprehensive modeling effort for the formation of DCAN, HAN4, and HAN6 (mono-chloroacetonitrile [MCAN], monobromoacetonitrile [MBAN], TCAN, DCAN, BCAN, and DBAN) during chlorination, chloramination, and prechlorination under UFC conditions. Multivariable predictive models were developed including several parameters such as UV_{254} , DOC, DON/DOC, $SUVA_{254}$, Br^- , oxidant dose, pH, contact time, and temperature for different water matrices (e.g., NOM, AOM, EfOM impacted waters, distribution system, and groundwater). Furthermore, this study evaluated the impact of pH on the correlation of HAN4/HAN6 vs. THM4 formation during chlorination process.

2. Materials and methods

2.1. Data compilation

A comprehensive HAN database under UFC was collected from the existing literature in addition to our own laboratory results. The correlation matrix of independent variables was performed after the log transformation of variables for model development, since the log transformation can reduce or remove the skewness of the original dataset. The water quality parameters for chlorination, chloramination, and prechlorination data sets are presented in Tables S2, S3, and S4.

The formation dataset under chlorination conditions for DCAN (sample number, $n = 216$), HAN4 ($n = 208$) and HAN6 ($n = 142$) samples covered a range of UV_{254} (0.014–1.472 cm^{-1}), DOC (0.3–9.8 mg/L), Br^- concentration (0.0015–9 mg/L), pH (5.5–9), chlorine dose (0.5–10 mg/L), contact time (0.5–72 h), and temperature (16.5–21 °C). The database included the results for samples from different water sources including distribution systems ($n = 30$), groundwater sources ($n = 29$), EfOM samples from secondary effluents of different WWTPs ($n = 54$), laboratory-grown AOMs samples ($n = 38$) from different algal species, and isolated/natural NOMs samples ($n = 57$). Among all water sources, DON concentrations were only available for EfOM samples (ranging from 1.5 to 30.7 mg/L as N) (Table S2 in the SI section).

Because of the limited number of available chloramination and prechlorination datasets in the literature, the chloramine dataset only included isolated/natural NOMs samples ($n = 35$) with a range of DOC

Table 1
Literature review on predictive models for formation of HANs.

No	Source Type	Oxidant Type	Testing Condition	DBPs	n	Bromide range (mg/L)	Modeling Approach	References	
1	Distribution systems	Chlorination	Samples were collected from the distribution system and analyzed	HAN4	300		Linear Mixed Regression	Guilherme and Rodriguez, 2017	
2				DCAN	NR		Linear Mixed and Generalized Linear Mixed Models	Chhipi-Shrestha et al., 2018	
3				HAN4	NRNR		Multivariate Linear Regression	Mian et al., 2020	
4	Raw water	Chlorination	FP	DCAN	40	0–0.25	Pearson Correlation	Kolla, 2004	
5	WWTP, DWTP, Groundwater, River and jar test samples			DCAN	190		F-test, Student's T-test, and Multiple Linear Regression	Chen and Westerhoff, 2010	
6	2 WTPs			HAN4	166	0–1	Multiple Linear Regression, Backward Stepwise Regression, Pearson Correlation and Sensitivity Analysis	Bergier et al., 2017	
7	Reservoir, River and Lake	Chloramination		HAN4	154	0.3–0.6	Multiple Linear Regression	Lin et al., 2018	
	Distribution systems, Groundwater, EfOM and AOM impacted, and NOM AOM impacted water			DCAN	32				
8		Chlorination	UFC	HAN4	33	0–0.4	Multiple Linear Regression	This study	
		Chloramination		DCAN	216				
				HAN4	208	0–10			
				HAN6	142				
		Prechlorination		DCAN	35		Multiple Linear Regression		
				HAN4	51	0–0.4			

FP: Formation Potential, UFC: Uniform Formation Condition, n: number of samples used in model development, NR: Not Reported, WWTP:Wastewater treatment plants, DWTP:Drinking water treatment plants, EfOMs:Effluent organic matters, AOMs:algal organic matters, NOMs:natural organic matters.

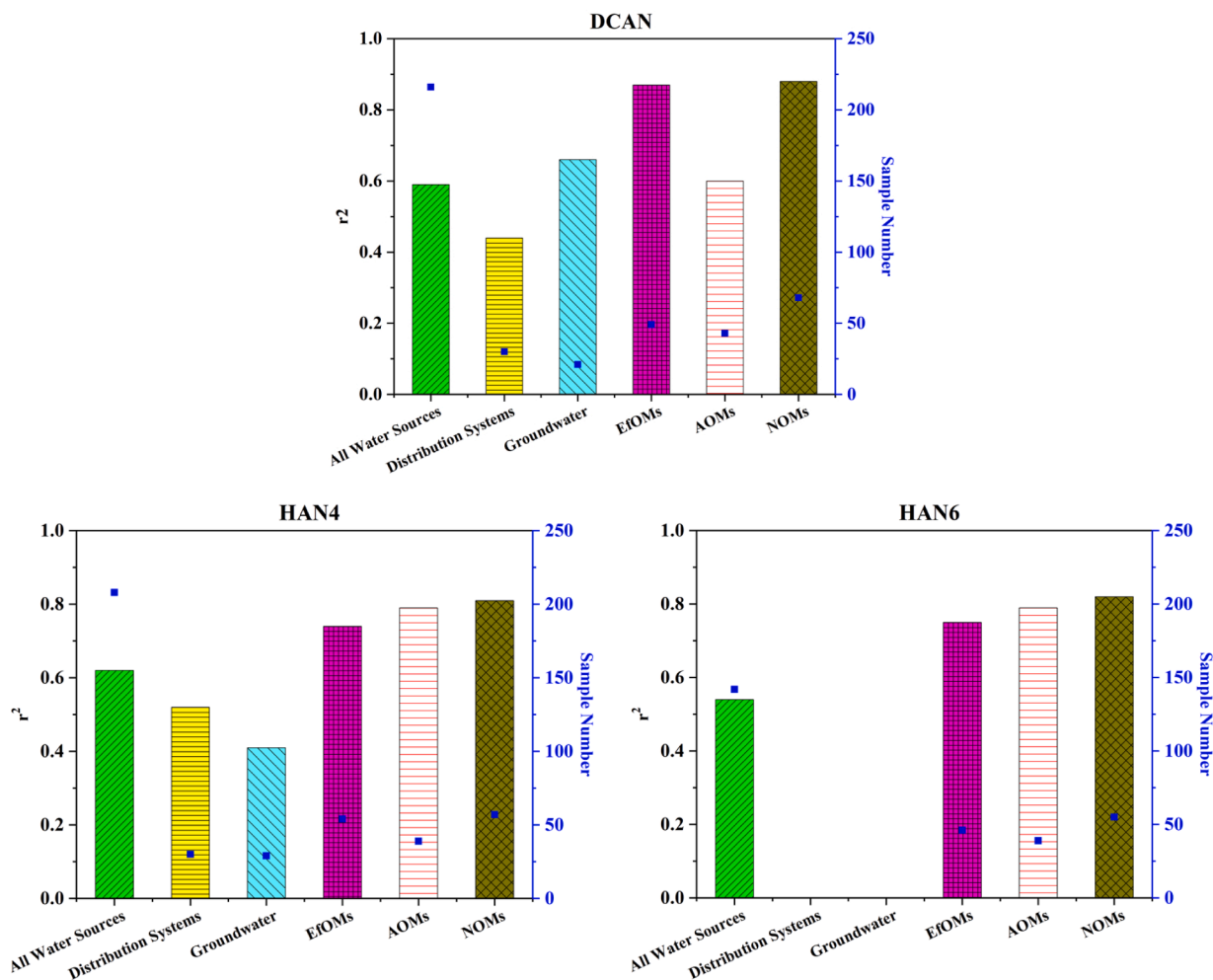


Fig. 1. Effect of water sources on the prediction models for DCAN, HAN4 and HAN6 formation in the presence of free chlorine. 'EfOMs:Effluent organic matters, AOMs:algal organic matters, NOMs:natural organic matters.

(2–5.4 mg/L), Br[−] (0–0.5 mg/L), pH (4–7.5), chloramine dose (2.3–8 mg/L as Cl₂), contact time (5–72 h), and temperature (10–30 °C). On the other hand, the dataset for chlorination followed by chloramination (Cl₂—NH₂Cl process: prechlorination followed by ammonia addition) for AOM impacted waters, is obtained from Liu et al., 2019. Prechlorination dataset only included formation of HAN4 ($n = 56$) from laboratory-grown AOMs samples at room temperature (21 °C) and a range of DOC (0.5–4 mg/L), Br[−] (0–0.4 mg/L), pH (6.5–8), prechlorination time (0.5–30 mins) and dose (1.3–7 mg/L as Cl₂), and temperature.

2.2. Predictive model equations

A multivariable equation (Equation, eq. 1), which includes water quality (UV₂₅₄, DOC, and Br[−]) and operational parameters (pH, oxidant dose, contact time, and temperature), was employed for statistical prediction of HAN formation. The predictive model has the following form:

$$\begin{aligned} \text{logHANs} = & a(\text{logUV}_{254}) + b(\text{logDOC}) + c(\text{logBr}^{-}) + d(\text{logpH}) \\ & + e(\text{logOxidant dose}) + f(\text{logTime}) + g(\text{logTemperature}) + h \end{aligned} \quad (1)$$

In this model, UV₂₅₄ (cm^{−1}), DOC (mg/L), Br[−] (mg/L), pH, oxidant dose (mg/L), time (hour) and temperature (°C) are the independent

variables, while HANs (mg/L) is the dependent variable. The coefficients "a", "b", "c", "d", "e", "f", and "g" are the regression coefficients, and "h" is the regression constant. Eq. (1) was employed for the prediction of HAN formation in all tested water sources (except EfOM and AOM during chlorination). For the EfOM model, the ratio of DON/DOC term was used in the predictive model formula instead of only DOC because the DON data was available. For the AOM impacted waters, SUVA₂₅₄ term was used in the model, instead of UV₂₅₄ and DOC, due to the constant DOC concentrations (2 mg/L) in the AOM dataset. The coefficients "i" and "j" are the regression coefficients of DON/DOC and SUVA₂₅₄, respectively.

The equation terms considered water quality and operational parameters that have been shown to influence the formation of HANs during chlorination, chloramination, and prechlorination (Liu et al., 2019; Bond et al., 2011; Dotson et al., 2009). Previous experimental studies showed that increasing DOC, Br[−], oxidant dose, contact time, and temperature positively correlate with HAN formation, while pH negatively correlates and decreases the formation of HANs (Chu et al., 2010; Glezer et al., 1999; Hua et al., 2006; Liu et al., 2018; Xue et al., 2014; Yang et al., 2008). In a study conducted by Lee et al. (2007), authors reported that wastewater sources (with high DON contents [0.18–0.27 mg/L]) containing amino sugars (0.22 nmol/mg of DOC) and proteins (0.82 nmol/mg of DOC) showed higher DCAN yields upon chlorination. Likewise, Huo et al. (2013) showed that more than 80% of

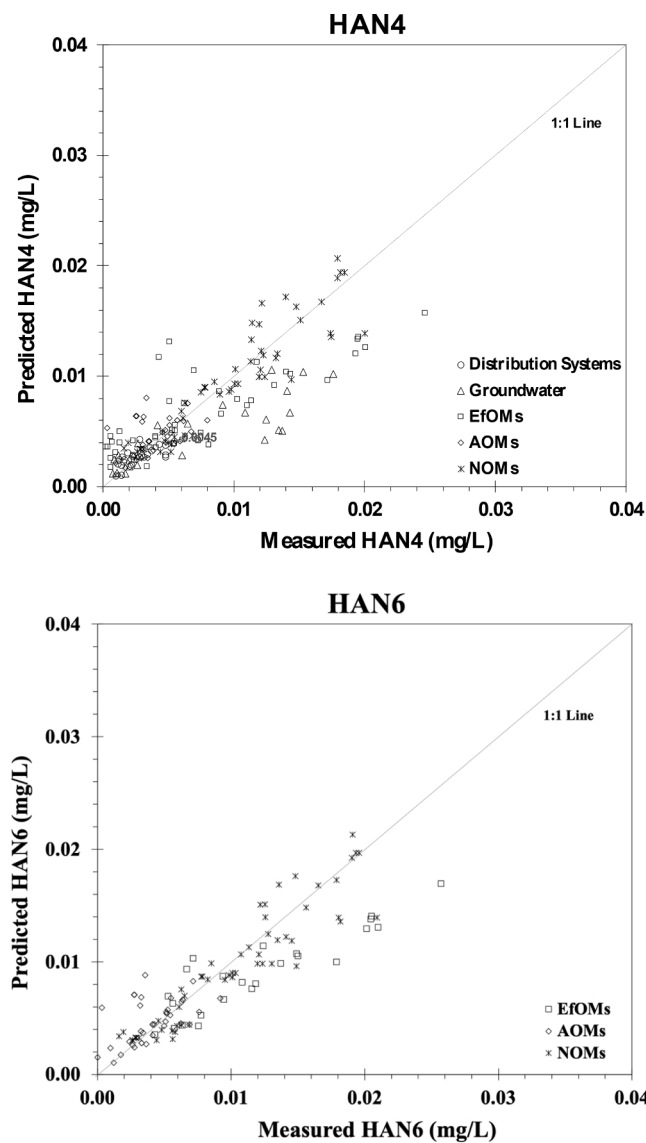


Fig. 2. Modeling data vs. measured data of HAN4 and HAN6 formation in different water sources.

DON in wastewater effluents contains hydrophilic moieties (low SUVA₂₅₄). Therefore DON is expected to serve as potential precursors for HAN formation, and it was included in the EfOM model.

2.3. Statistical data analysis

The development of model equations was accomplished by performing MLR analysis. All statistical analysis results were conducted by SAS v.9.3 software. The generalized linear model (GLM) procedure of SAS was applied for parameter selection. The MLR analysis was used to develop correlations between water quality and operational parameters, and HAN formation. Regression assumption was evaluated with a linear relationship for describing a straight-line relationship between independent and dependent variables. Therefore, the linear relationship between the independent variables (water quality and operational parameters) and the dependent variable (HAN formation) was examined side-by-side.

The linearity of the model equations was examined by the coefficient of determination (r^2). The regression models were checked by p -values, assessed with the analysis of variance (ANOVA). A small p -value ($\leq .05$) indicates strong evidence that at least one of the independent variables

of the developed equation is significantly important to predict the dependent variable. The intercorrelations of independent variables were controlled by the variation inflation factor (VIF). VIF value is the reciprocal of the tolerance value, and their small values ($VIF < 4$) indicate low correlation among variables under ideal conditions. As VIF values higher than 10, this may suggest that there is a problem with multicollinearity (Hair et al., 2010). The predictive performance of models was also estimated with percent difference between measured and predicted values (Mian et al., 2020). While root mean squared error (RMSE) was used as a measure of external validation data, the predictive precision for models evaluated by prediction error sum of squares (PRESS). A detailed explanation of the multiple regression modeling technique can be found in our previous publications (Ersan et al., 2016; 2019; Apul et al., 2020; Croue and Roux, 2011)

3. Results and discussion

3.1. The prediction of HAN formation during chlorination

Since the mass- and molar-based models developed for DCAN, HAN4, and HAN6 were mostly in agreement, the mass-based model results were presented and discussed in this manuscript. The modeling variables (UV₂₅₄, DOC, Br⁻, pH, oxidant dose, contact time, and temperature) for DCAN, HAN4, and HAN6 during chlorination under UFC are presented in Table S2 in the SI section.

To examine the model correlations in different types of waters, HANs models were developed for each water type. The equations obtained for HAN4 formation in five different water sources are shown in Eqs. (2)–(7). The coefficient of determinations (r^2) is the key output of regression analysis to evaluate the developed models for HANs formation. The r^2 values of the HANs model were, in general, higher in the individual types as compared to the cumulative analysis of the data eq (2)–(7). The r^2 values of HAN4 models of NOM, AOM, and EfOM impacted waters were within the range of 74–81%, which indicated the suitability of models for predicting HAN formation. On the other hand, the r^2 values of HAN4 models for both groundwater and distribution systems were lower than those of other waters (52 and 41%, respectively). The lowest r^2 value observed for distribution systems may be attributed to varying water quality conditions and complex operating conditions. Besides, when all water types were included in the prediction model, the r^2 value was lower than individual water types (except distribution systems). The cumulative models developed including only NOM, AOM and EfOM data still resulted lower r^2 values (DCAN model r^2 : 0.59, HAN4 model r^2 : 0.62, HAN6 model r^2 : 0.70) (data is not shown). This indicated that the characteristics of HAN precursors vary among these different type of organic matter. Therefore, the prediction modeling for individual water types has been shown to be more reliable than cumulative analysis of the HAN data in this study.

$$\begin{aligned} \log\text{HAN4}_{(\text{NOM})} = & -(0.11 \pm 0.05)\log\text{UV}_{254} + (0.37 \pm 0.41)\log\text{DOC} \\ & +(0.48 \pm 0.05)\log\text{Br}^- - (0.84 \pm 0.39)\log\text{pH} + (0.6 \pm 0.46)\log\text{ChlorineDose} \\ & +(0.19 \pm 0.12)\log\text{Time} - (19.23 \pm 3.29)\log\text{Temperature} + 23.2 \pm 4.34 \end{aligned} \quad (2)$$

($n : 57, r^2 : 0.8, p$ values : < .0001)

$$\begin{aligned} \log\text{HAN4}_{(\text{AOM})} = & (0.11 \pm 0.17)\log\text{SUVA}_{254} + (0.28 \pm 0.04)\log\text{Br}^- \\ & -(1.01 \pm 0.41)\log\text{pH} + (0.63 \pm 0.35)\log\text{ChlorineDose} \\ & +(0.35 \pm 0.05)\log\text{Time} - 2.19 \pm 0.43 \end{aligned} \quad (3)$$

($n : 39, r^2 : 0.79, p$ values : < .0001)

$$\begin{aligned} \log\text{HAN4}_{(\text{EfOM})} = & -(0.73 \pm 0.37)\log\text{UV}_{254} + (0.09 \pm 0.05)\log\text{DON/DOC} \\ & +(0.39 \pm 0.06)\log\text{Br}^- + (0.76 \pm 0.71)\log\text{pH} - 2.19 \pm 0.43 \end{aligned} \quad (3)$$

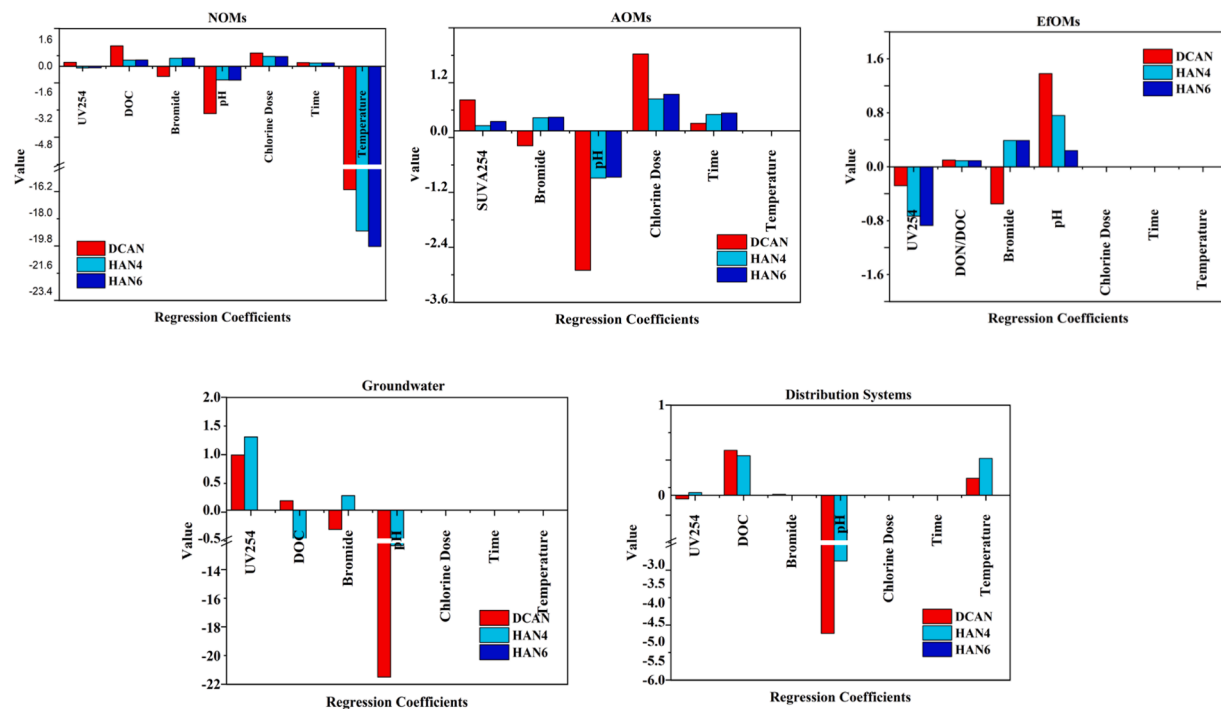


Fig. 3. The regression coefficients (UV₂₅₄, DOC concentration, bromide, pH, chlorine dose, time, and temperature) of the models developed for formation of DCAN, HAN4 and HAN6 in the presence of free chlorine in different water sources. Δ Value: the regression coefficients value of each variable, All sources: sum of the all water sources, EfOMs: Effluent organic matters, AOMs: Algal organic matters, NOMs: Natural organic matters.

$$(n : 54, r^2 : 0.74, p \text{ values} : < .0001) \quad (4)$$

$$\begin{aligned} \log\text{HAN4}_{(\text{Distribution Systems})} = & (0.03 \pm 0.2)\log\text{UV}_{254} \\ & + (0.44 \pm 0.3)\log\text{DOC} + (0.01 \pm 0.29)\log\text{Br}^- - (2.91 \pm 3.63)\log\text{pH} \\ & + (0.41 \pm 0.39)\log\text{Temperature} - 0.51 \pm 3.34 \end{aligned}$$

$$(n : 30, r^2 : 0.52, p \text{ values} : 0.01) \quad (5)$$

$$\begin{aligned} \log\text{HAN4}_{(\text{Groundwater})} = & (1.3 \pm 0.61)\log\text{UV}_{254} - (0.6 \pm 0.79)\log\text{DOC} + (0.26 \pm 0.13) \\ & \log\text{Br}^- - (12.16 \pm 5.62)\log\text{pH} + 10.64 \pm 5.22 \end{aligned}$$

$$(n : 29, r^2 : 0.41, p \text{ values} : 0.03) \quad (6)$$

$$\begin{aligned} \log\text{HAN4}_{(\text{All water sources})} = & (0.24 \pm 0.05)\log\text{UV}_{254} + (0.14 \pm 0.3)\log\text{DOC} \\ & + (0.38 \pm 0.04)\log\text{Br}^- - (0.52 \pm 0.45)\log\text{pH} \\ & + (0.62 \pm 0.26)\log\text{ChlorineDose} + (0.36 \pm 0.08)\log\text{Time} \\ & - (19.21 \pm 3.73)\log\text{Temperature} + 22.94 \pm 4.84 \end{aligned}$$

$$(n : 208, r^2 : 0.62, p \text{ values} : < .0001) \quad (7)$$

Table 2 summarizes all the model parameter coefficients along with statistical comparisons of DCAN, HAN4, and HAN6 formation in five different water sources. The impact of water source type on r^2 of models for DCAN, HAN4, and HAN6 formations are presented in Fig. 1. The r^2 values of the DCAN model were, in general, higher in the individual water types as compared with all water sources collectively. The r^2 values of HAN4 and HAN6 models of NOM, AOM, and EfOM impacted waters were within the range of 60–88%, while the r^2 values of HAN4 and DCAN models for both groundwater and distribution systems were lower, in the range of 41–66% (Fig. 1). When the predicted and measured data of HAN4 and HAN6 formation for different water sources was compared, the predicted HAN4 and HAN6 formation fitted well with their measured data in all water sources (especially for water sources with the highest r^2 values) (Fig. 2). Besides, the average

percentage difference (Δ) values between measured and predicted values from all models were less than 35% for each DCAN, HAN4 and HAN6 formations in the different water sources (Table 2).

The values for all the model parameter coefficients of DCAN, HAN4, and HAN6 formation from different water sources are shown in Fig. 3. Among all variables, pH parameter was negatively correlated with HAN formation in the distribution system, groundwater, AOM, and NOM samples. Previous studies showed increasing pH decreased the formation of HANs due to base-catalyzed hydrolysis (Singer et al., 1995; Heller-Grossman et al., 1999; Reckhow et al., 2001; Na and Olson, 2004). However, pH showed an inverse relationship in the EfOM impacted water, resulting in an increased formation of HANs with increasing pH. The calculated pH coefficients for EfOM impacted water model were consistent with a previous study, where chlorination of secondary effluent waters at high pH led to an increased formation of some of the HANs, while an opposite trend was observed for the other water sources (Doederer et al., 2013). The observed positive correlation may be associated with the characteristics of EfOM impacted water samples, which may contain a mixture of precursors including NOM, AOM, and soluble microbial products (SMP) excreted during biological wastewater treatment processes as well as other anthropogenic compounds. Further data for the formation of HAN in wastewater effluents under UFC conditions is needed.

Due to the lack of available temperature data for different water sources in the literature, the temperature impacts on HAN formation were only examined for distribution systems and NOM waters. Temperature showed a positive correlation in the chlorinated humic acid samples, when temperature were increased from 4 to 15 °C. On the other hand, DCAN formation decreased with increasing temperature from 25 to 50 °C (Zhang et al., 2013). However, the formation of HANs in the NOM water samples exhibited a different behavior; the absolute value of temperature for NOM water was the most predominant descriptor and was negatively correlated with HAN formation (Fig. 3). The formation rates of DCAN, HAN4, and HAN6, and their decomposition rates could be enhanced with increasing temperature during chlorination of NOM waters. Another study concluded that increasing temperature enhanced

Table 2 Prediction model parameters for DCAN, HAN4 and HAN6 formation in the presence of free chlorination in different water sources.

Type of Sources	HANS	UV _{254(a)}	±	DOC(b)	±	SUVA _{254(j)}	±	DON /DOC (i)	±	Br ⁻ (c)	±	pH(d)	±	Oxidant Dose (e)	±	Time(f)	±	Temp (g)	±	h	±	n	r ²	Δ (%)	p values
NOMs	DCAN	0.24	0.07	1.24	0.5			-0.62	0.08	-2.88	0.74	0.8	0.56	0.22	0.15	-16.4	4.46	20	5.73	68	0.88	-6.1	<.0001		
	HAN4 _(eq,2)	-0.11	0.05	0.37	0.41			0.48	0.05	-0.84	0.39	0.6	0.46	0.19	0.12	-19.23	3.29	23.2	4.34	57	0.81	-8.5	<.0001		
	HAN6	-0.1	0.05	0.38	0.42	0.66	0.33	0.5	0.05	-0.85	0.4	0.59	0.47	0.2	0.13	-20.29	3.35	24.6	4.42	55	0.82	2.9	<.0001		
AOMs	DCAN							-0.32	0.08	-2.98	0.97	1.64	0.65	0.16	0.09	-1.91	0.97	43	0.60	22.2	<.0001				
	HAN4 _(eq,3)							0.28	0.04	-1.01	0.41	0.63	0.35	0.35	0.05	-2.19	0.43	39	0.79	-3.3	<.0001				
	HAN6							0.29	0.05	-0.99	0.43	0.78	0.37	0.38	0.05	-2.31	0.46	39	0.79	-6.9	<.0001				
EfOMs	DCAN	-0.28	0.32			0.1		0.04	-0.55	0.05	1.38	0.62			-5	0.61	49	0.87	26.4	<.0001					
	HAN4 _(eq,4)	-0.73	0.37			0.09		0.05	0.39	0.06	0.76	0.71			-3.15	0.71	54	0.74	-27.5	<.0001					
	HAN6	-0.87	0.37			0.09		0.05	0.39	0.06	0.24	0.7			-2.8	0.69	46	0.75	-37.1	<.0001					
DS	DCAN	-0.04	0.21	0.5	0.31			0.01	0.31	-4.79	3.84			0.19	0.41	1.21	3.54	30	0.44	35	0.05				
	HAN4 _(eq,5)	0.03	0.2	0.44	0.3			0.01	0.29	-2.91	3.63			0.41	0.39	-0.51	3.34	30	0.52	33.3	0.01				
	HAN6							-0.34	0.17	-21.48	10.38					20.42	9.76	21	0.66	-8.1	0.01				
GW	DCAN	0.98	0.9	0.177	1.28			0.26	0.13	-12.16	5.62					10.64	5.22	29	0.41	0.01	0.03				
	HAN4 _(eq,6)	1.3	0.61	-0.6	0.79																				
	HAN6																								
All water sources	DCAN	-0.94	0.1	3.67	0.57			-0.13	0.09	-0.97	0.96	-1.09	0.43	-0.14	0.17	-41.4	7.85	50.81	10.16	216	0.59	-8.3	<.0001		
	HAN4 _(eq,7)	0.24	0.05	0.14	0.3			0.38	0.04	-0.52	0.45	0.62	0.26	0.36	0.08	-19.21	3.73	22.94	4.84	208	0.62	-13.2	<.0001		
	HAN6	0.004	0.001	0.001	0.01			0.007	0.0008	-0.005	0.009	0.01	0.005	0.004	0	-0.32	0.08	0.43	0.1	1.42	0.54	-11.7	<.0001		

The coefficients “a”, “b”, “c”, “d”, “e”, “f”, “g”, “i”, and “j” are the regression coefficients of the each independence variables. h: the sample number, n: the sample number, ±:Standard errors, Temp.: Temperature, gray colored: not available data, All water sources: sum of the all water sources, EfOMs: Effluent organic matters, AOMs:Natural organic matters, DS: Distribution Systems, GW:Groundwater. Δ = estimated individual difference in the percentage between the measured and predicted value: $\{\Delta\} = (\text{MV-PV})/\text{MV} \times 100$; MV = measured value, PV = predicted value (Mian et al., 2020).

the decomposition rates of DCAN (Nikolaou et al., 2004).

When more brominated species were included within the models, the impact of Br⁻ and chlorine dose on the model equations increased for all water sources (Fig. 3). When the HAN speciation shifted from chlorinated to chloro/bromo and/or brominated HANs, as a result of an increase in Br⁻ concentration, (i.e., from DCAN to BCAN and DBAN), the Br⁻ contribution in the model equation became more apparent (DCAN to HAN6 in Table 2). Therefore, the model results clearly showed that increasing Br⁻ concentration shifted the speciation to more brominated HANs, and increasing chlorine dose increased the decomposition of HANs (Chow et al., 2011; Soyluoglu et al., 2020; Hua et al., 2006). For the UV₂₅₄, a negative correlation was only observed in EfOM impacted waters. The SUVA₂₅₄ parameter within the DCAN, HAN4, and HAN6 model equations of AOM impacted showed a positive correlation with HAN formation. On the other hand, DOC parameter showed different impact on the model equations for different water sources (Table 2). DON/DOC ratios in EfOM impacted waters were positively correlated with DCAN, HAN4, and HAN6 modelings supporting that DON can be a significant source of HAN precursors (Westerhoff and Mash, 2002; Lee et al., 2007). On the other hand, increasing contact time during chlorination increased HAN formation in both NOM and AOM impacted waters. It should be noted that the dataset for HAN6 under UFC conditions is much smaller as compared to DCAN and HAN4 in the literature. When all data were modeled together, the prediction strength of each regression coefficients (r^2) decreased (Table 2). This is due to weaker correlations of distribution systems and groundwater systems as well as the difference in the nature of HAN precursors in different waters.

Overall, in the presence of free chlorine, the r^2 values, which is the indicator of the prediction model strengths, highly depends on the availability of HAN formation dataset, including the number of DCAN, HAN4, and HAN6, independent variables (UV₂₅₄, DOC, Br, pH, dose, contact time and temperature) and type of water sources. Reporting complete HAN6 speciation data sets with several water quality parameters (especially including DON and DOC together) will be valuable to further advance the HAN modeling efforts. Furthermore, DON values will be valuable for modeling of other nitrogenous DBPs that may be measured during the same studies.

3.2. The prediction of HAN formation during chloramination

The modeling variables (DOC, pH, oxidant dose, contact time, and temperature) that are used for developing a predictive model for DCAN

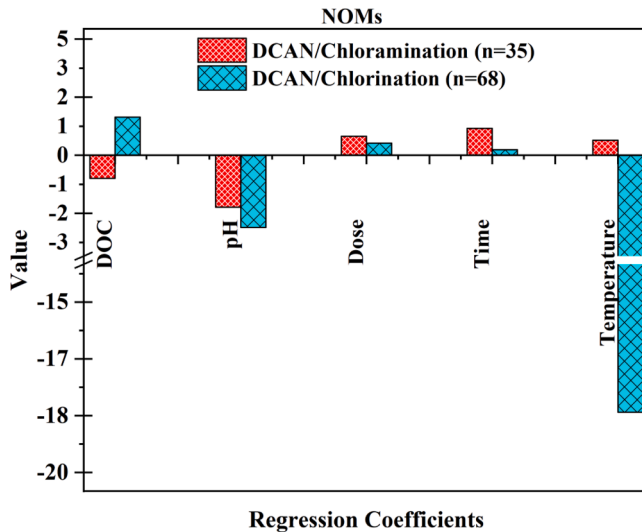


Fig. 4. Effect of oxidant types on the prediction models for DCAN formation in NOM waters. ‘value’: the regression coefficients value of each variable, n: the sample number.

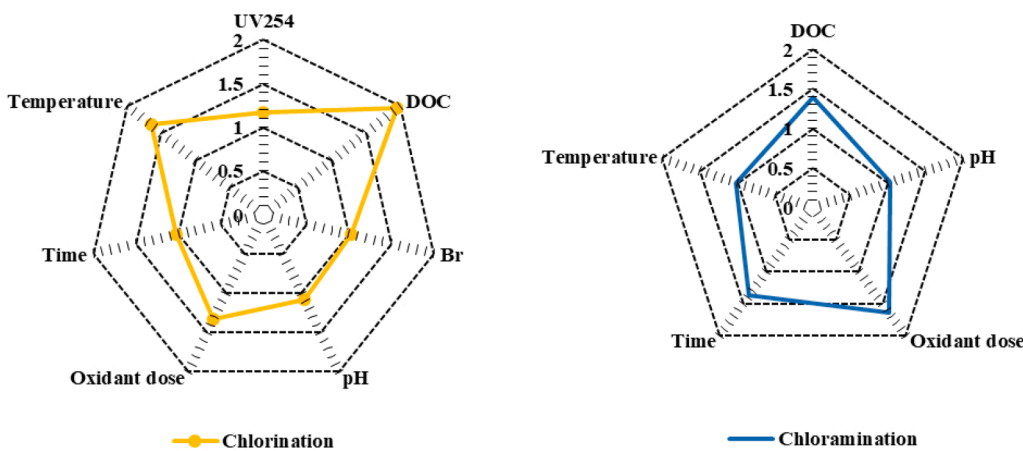


Fig. 5. The variation inflation factor (VIF) values for model of DCAN formation during chlorination and chloramination.

in the presence of chloramine under UFC are compiled in Table S3 in the SI section. Due to limited number of studies in the literature, which includes all the investigated model parameters in this study, the predictive modeling for chloramination was only evaluated for DCAN formation in the NOM water samples.

$$\begin{aligned} \log DCAN = & -(0.91 \pm 1.21) \log DOC - (2.06 \pm 1.52) \log pH \\ & + (0.75 \pm 0.39) \log ChloramineDose + (1.06 \pm 0.34) \log Time \\ & + (0.59 \pm 1.29) \log Temperature - 0.93 \pm 2.49 \end{aligned} \quad (5)$$

The r^2 value of model variables and coefficients for DCAN formation in NOM water samples are given in Eq. (5) and shown in Fig. 4. Among all descriptors, the pH term has a negative correlation in the chloramination model due to the base-catalyzed decomposition of DCAN (Roux and Croue, 2012; Croue and Roux, 2011; Yu and Reckhow, 2015). Increasing pH enhanced the degradation rates of DCAN, which has been observed in previous studies (Ersan et al., 2019b; Lee and Westerhoff, 2009; Yang et al., 2007). On the other hand, except the DOC term, chloramine dose, contact time, and temperature terms for DCAN formation showed positive correlations, which is in agreement with

previous studies where the formation of DCAN increased with increasing chloramine dose, contact time, and temperature (Nikolaou et al., 2004; Reckhow et al., 2001; Yang et al., 2007).

In terms of the impact of oxidant type (chlorine vs. chloramine) on the modeling of DCAN formation, the r^2 value of DCAN formation modeling under chloramination ($r^2=0.49$, $n=35$) was lower than during chlorination ($r^2=0.88$, $n=68$). This was attributed to narrower independent variable ranges for chloramination dataset, shown in Fig. S3, which impacted the prediction strength of the model. The values for all model parameter coefficients of DCAN formation in NOM water are presented in Fig. 4. The trends of regression coefficient values (DOC, pH, oxidant dose, time, and temperature) for both chlorination and chloramination datasets were slightly different. Among all variables in Fig. 4, the pH parameter for both oxidants showed negative correlation with DCAN formation in surface waters. On the other hand, temperature term was also negatively correlated with DCAN formation under chlorination, which may be due to enhanced decomposition rates of DCAN at increasing temperatures (Nikolaou et al., 2004; Reckhow et al., 2001). For the chloramination dataset, the temperature parameter showed a positive correlation in the NOM samples. It should be noted that the temperature parameter for chloramination dataset (10–25 °C) was much narrower than chlorination (4–50 °C) (Table S2 and S3 in the SI section); thus the modeling of DCAN formation under varying temperature conditions warrants further investigation during chloramination process. It has been also shown that increasing DOC concentration, oxidant dose, and contact time in chlorination and chloramination increased DCAN formation. However, the regression coefficients of the chlorination dataset are less impacted than the chloramination dataset, when each parameter was compared according to the oxidant type. This difference can be attributed to the less stability of DCAN in the presence of free chlorine versus monochloramine. The modeling of HAN formation under UFC warrants further investigation when more chloramination data becomes available in the literature.

To better visualize the multicollinearity, the change in VIF values during HAN formation modeling for chlorination and chloramination is shown by using a radar chart in Fig. 5 and Fig. S1. Among all variables, while the VIF value for DOC term in chlorination (VIF=1.95) was higher, during chloramination VIF value was higher for the oxidant dose (VIF=1.4) as compared to other variables. Besides, the VIF value for temperature term was higher during chlorination (VIF=1.66) than chloramination (VIF=1). But, multicollinearity (VIF>10) was not observed for both chlorine and chloramine datasets (Fig. S5-S6 in the SI section).

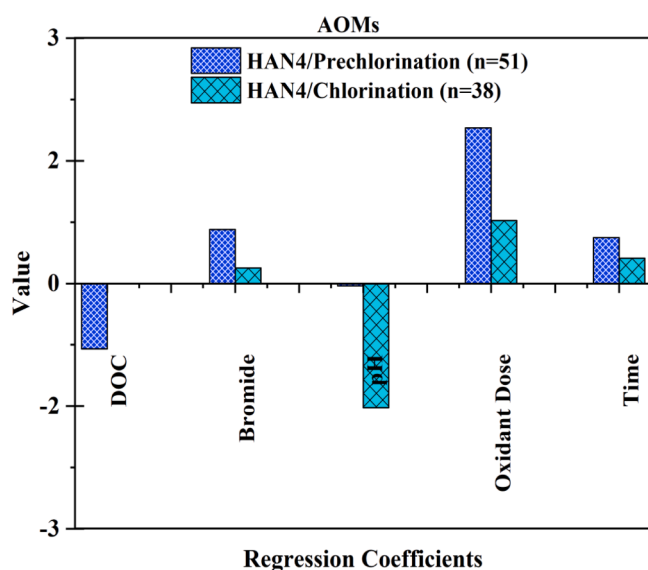


Fig. 6. Comparison of prechlorination and chlorination process for the prediction models of HAN4 formation in AOMs impacted waters. 'value': the regression coefficients value of each variable, n: the sample number.

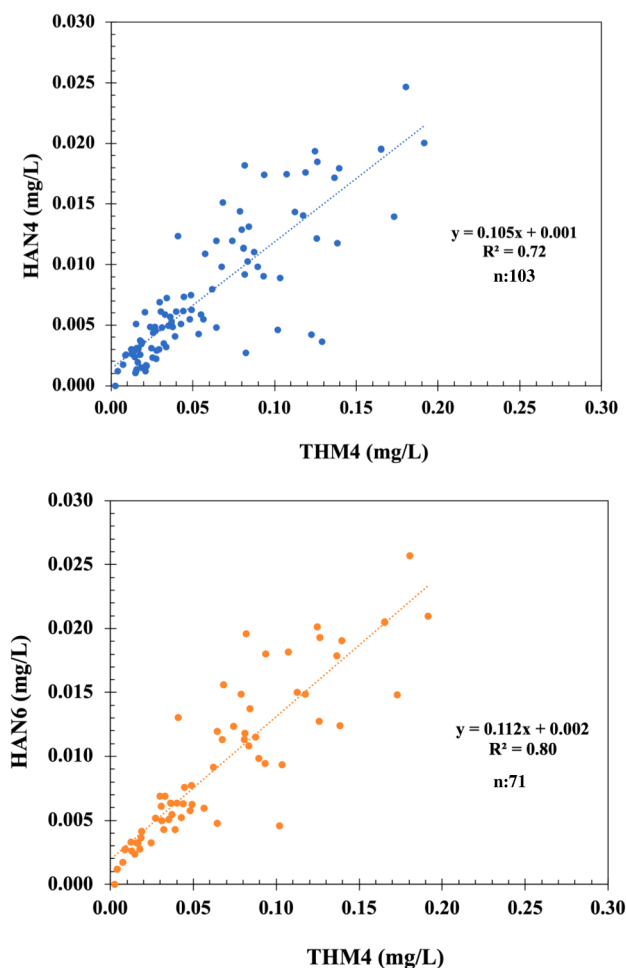


Fig. 7. The correlation of HANs vs. THMs during chlorination process at pH 7–8.

3.3. The prediction of HAN formation during prechlorination/chloramination

The modeling variables (DOC, pH, Br⁻ concentration, prechlorination time and prechlorination dose) for prechlorination/chloramination that were used for developing a predictive model for HAN4 under UFC were compiled in Table S4 in the SI section. Due to the limited number of prechlorination/chloramination datasets with all parameter values for HAN4 formation in the literature, predictive modeling was only examined for AOM impacted waters. The r^2 value of model variables and coefficients for HAN4 formation during prechlorination/chloramination in AOM impacted water samples were given in Eq. 6.

$$\begin{aligned} \text{logHAN4} = & -(0.80 \pm 0.95)\text{logDOC} + (0.75 \pm 0.39)\text{logBr} \\ & + (-0.03 \pm 0.78)\text{logpH} \\ & + (0.56 \pm 0.05)\text{logPrechlorinationTime} \\ & + (1.90 \pm 1.12)\text{logPrechlorinationDose} - 1.49 \pm 0.67 \end{aligned} \quad (6)$$

(n : 51, r^2 : 0.83, p values : < .0001)

Among all independent variables, prechlorination dose was the most influential parameter (p -values <0.0001), and positively correlated with HAN formation in the AOM impacted waters. While DOC and pH terms were negatively correlated in the prechlorination process, as shown in Fig. 6., Br⁻ and prechlorination contact time for HAN4 formation showed positive correlations. This suggests that the formation of HAN4

increased with increasing prechlorination dose, contact time and initial Br⁻ concentration, which agrees well with previous research (Tian et al., 2013).

Since there is no full dataset available for HANs formation during chloramination in AOM impacted waters, the prechlorination/chloramination process was compared with only the chlorination model in AOM impacted waters. The model prediction of HAN4 during prechlorination/chloramination ($r^2=0.83$, $n=51$) was slightly higher than chlorination process ($r^2=0.76$, $n=38$). With increasing chlorine contact times in both prechlorination/chloramination and chlorination processes, the formation of HAN4 declined with increasing pH due to lower stability of HANs under alkaline conditions (Yu and Reckhow et al., 2015; Liu et al., 2018). In contrast to chlorination, a lesser pH impact was observed on the HAN4 model in prechlorination/chloramination (Fig. 6). This may be due to narrower pH ranges used in the prechlorination/chloramination dataset (Table S4 in the SI section), which may have influenced the prediction strength of the model. Meanwhile, the formation of HAN4 in the prechlorination/chloramination process increased with increasing Br⁻ concentration (Fig. 6). This finding was in agreement with HAN4 formation results reported by Tian et al. (2013) and Liu et al. (2019).

3.4. HANs vs. THMs correlations

Since THM data was available for the HAN datasets, the correlations between HAN and THM formation were also examined. However, pH is an important parameter in this analysis because with increasing pH, the formation of THMs is enhanced due to the base-catalyzed reactions, whereas at high pH conditions (i.e., pH> 8) HANs undergo base-catalyzed hydrolysis (Reckhow et al., 2001; Yu and Reckhow, 2015; Ersan et al., 2019a; Hua and Reckhow, 2006; Reckhow et al., 1990).

Among all pH ranges, HAN4 vs. THM4 ($y = 0.1047x+0.0014$, $r^2:0.72$, $n:103$), and HAN6 vs. THM4 ($y = 0.1118x+0.002$, $r^2:0.80$, $n = 71$) was found highly correlated in the pH range of 7 to 8 of chlorination (Fig. 7). At higher pH levels (pH> 8.0), the correlations between HANs and THMs decreased (Table S8 in the SI section) which was attributed to hydrolysis of HANs (Singer et al., 1994; Reckhow 2001). When THMs vs. HANs correlations were performed in individual water sources (distribution systems, groundwater, EfOM, AOM, and NOM waters) under similar pH ranges (7–8), THMs highly correlated with HANs in distribution system, EfOM and AOM impacted waters ($r^2:0.62\text{--}0.91$) (Table S9 in the SI section). Due to the limited data sets for each water sources, pH impacts on the correlation between HAN4/HAN6 vs. THM4 was not individually evaluated in this study. On the other hand, when the data for all pH values analyzed together, the correlation coefficient (r^2) was 0.52 for both HAN4 vs. THM4, HAN6 vs. THM4 correlations (Table S8 in the SI section). Therefore, these results show that pH is an important parameter for both HAN formation prediction as well as developing THM vs. HAN correlations. At pH 7–8 range, HAN formation on a mass basis was approximately 10% of THM formation.

4. Conclusions

Poly-parameter (UV₂₅₄, DOC, DON/DOC, SUVA₂₅₄, Br⁻, oxidant dose, pH, contact time, and temperature) model equations were developed for the prediction of HANs formation in distribution system conditions during chlorination, chloramination, and prechlorination/chloramination processes. This comprehensive analysis showed that:

- The type of water source during chlorination influenced the linearity (r^2) of the model equations. The r^2 values for the DCAN model were mostly higher in the individual types (except distribution systems) as compared to the cumulative analysis of the data. This was attributed to differences in HAN precursor characteristics. The r^2 values of HAN4 and HAN6 models of NOM, AOM, and EfOM impacted waters were within the range of 60–88%, which indicated the success of the

- models in predicting HAN formations. On the other hand, the r^2 values of HAN4 models for both groundwater and distribution systems were within the range of 41–66%.
- Among all variables, pH was the most significant descriptor (p -values <.0001) for DCAN, HAN4, and HAN6 in the chlorination process, and inversely affected the HAN formation in the distribution system, groundwater, AOM, and NOM waters. On the contrary, increasing pH positively affected the formation of HAN in the EfOM impacted water.
 - A positive correlation between DON/DOC term and DCAN, HAN4 and HAN6 models observed in EfOM impacted waters indicated the role of organic nitrogen species in wastewater effluent. However, DON concentrations has not been reported for other types of waters. Therefore, reporting both DOC and DON in DBP studies is important for future modeling efforts of nitrogenous DBPs.
 - For chloramination, pH was the significant parameter, and it was negatively correlated with DCAN formation in NOM waters.
 - The model prediction of DCAN during chlorination was higher ($r^2=0.88$, $n = 68$) than chloramination ($r^2=0.49$, $n = 35$), which is attributed to the higher HAN stability in the presence of chloramine.
 - For prechlorination/chloramination, prechlorination dose was the most influential parameter (p -values <.0001), which was positively correlated with HAN formation in the AOM impacted waters. The model prediction of HAN4 formation in prechlorination/chloramination ($r^2=0.83$, $n = 51$) was higher than chlorination ($r^2=0.76$, $n = 38$).
 - pH is an important parameter while examining THM vs. HAN correlations. Among all pH ranges, the pH range of 7 to 8 showed the highest correlation between HAN4 and THM4 ($r^2:0.72$), and HAN6 and THM4 ($r^2:0.80$) during chlorination. At this pH range, HAN formation was approximately 10% of HAN4 and HAN6 formation on a mass basis.
 - Future papers providing the values for all model parameters (especially DON and DOC) listed above along with HAN formation and speciation will help to create larger and more complete datasets, and advance the predictive modeling of HANs as well as other nitrogenous DBPs.

Declaration of Competing Interest

The authors declare that they have no known competing financial interests or personal relationships that could have appeared to influence the work reported in this paper.

Supplementary materials

Supplementary material associated with this article can be found, in the online version, at doi:[10.1016/j.watres.2021.117322](https://doi.org/10.1016/j.watres.2021.117322).

References

- Apul, O.G., Perreault, F., Ersan, G., Karanfil, T., 2020. Linear solvation energy relationship development for adsorption of synthetic organic compounds by carbon nanomaterials: an overview of the last decade. *Environ. Sci.: Water Res. Technol.* 6, 2949–2957.
- Bergier, T., Kowalewski, Z., Gruszczyński, S., 2017. Modeling and predicting the concentration of volatile organic chlorination by-products in Krakow drinking water. *Environ. Eng.* 71–82.
- Bond, T., Huang, J., Templeton, M.R., Graham, N., 2011. Occurrence and control of nitrogenous disinfection by-products in drinking water e A review. *Water Res* 45, 4341–4354.
- Bougeard, C.M.M., Goslan, E.H., Jefferson, B., Parsons, S.A., 2010. Comparison of the disinfection by-product formation potential of treated waters exposed to chlorine and monochloramine. *Water Res* 44, 729–740.
- Chen, B., Westerhoff, P., 2010. Predicting disinfection by-product formation potential in water. *Water Res* 44, 3755–3762.
- Chow, A.T., Geen, A.T.O., Dahlgren, R.A., Díaz, F.J., Wong, K., Wong, P., 2011. Reactivity of Litter Leachates from California Oak Woodlands in the Formation of Disinfection By-Products. *J Environ Qual* 1607–1616.
- Chowdhury, S., Champagne, P., Mclellan, P.J., 2009. Models for predicting disinfection byproduct (DBP) formation in drinking waters : a chronological review. *Sci. Total Environ.* 407, 4189–4206.
- Chowdhury, S., Rodriguez, M.J., Serodes, J., 2010. Model development for predicting changes in DBP exposure concentrations during indoor handling of tap water. *Sci. Total Environ.* 408, 4733–4743.
- Chu, W., Gao, N., Deng, Y., 2010. Formation of haloacetamides during chlorination of dissolved organic nitrogen aspartic acid. *J Hazard Mater.* 173, 82–86.
- Chhipi-Shrestha, G., Rodriguez, M., Sadiq, R., 2018. Framework for cost-effective prediction of unregulated disinfection by-products in drinking water distribution using differential free chlorine. *Environ. Sci. Water Res. Technol.* 4 (10), 1564–1576.
- Croué, J., Roux, J.L., 2011. Chloramination of nitrogenous contaminants (pharmaceuticals and pesticides): NDMA and halogenated DBPs formation. *Water Res* 45 (10), 3164–3174.
- Doederer, K., Gernjak, W., Weinberg, H.S., Jose, M., 2013. Factors affecting the formation of disinfection by-products during chlorination and chloramination of secondary effluent for the production of high quality recycled water. *Water Res* 1 (48), 218–228.
- Dotson, A., Westerhoff, P., Krasner, S.W., 2009. Nitrogen enriched dissolved organic matter (DOM) isolates and their affinity to form emerging disinfection. *Water Sci Technol* 60 (1), 135–143.
- Engerholm, B.A., Amy, G.L., 2017. A predictive model for chloroform formation from humic acid. *J Am Water Works Assoc* 75, 418–423.
- Ersan, G., Apul, O.G., Karanfil, T., 2019. Predictive models for adsorption of organic compounds by Graphene nanosheets: comparison with carbon nanotubes. *Sci. Total Environ.* 654, 28–34.
- Ersan, G., Apul, O.G., Karanfil, T., 2016. Linear solvation energy relationships (LSER) for adsorption of organic compounds by carbon nanotubes. *Water Res* 98, 28–38.
- Ersan, M.S., Liu, C., Amy, G., Karanfil, T., 2019a. The interplay between natural organic matter and bromide on bromine substitution. *Sci. Total Environ.* 646, 1172–1181.
- Ersan, M.S., Liu, C., Amy, G., Plewa, M.J., Wagner, E.D., Karanfil, T., 2019b. Chloramination of iodide-containing waters: formation of iodinated disinfection byproducts and toxicity correlation with total organic halides of treated waters. *Sci. Total Environ.* 697, 134–142.
- Feungpean, M., Panyapinyopol, B., Elefsiniotis, P., 2015. Development of statistical models for trihalomethane (THM) occurrence in a water distribution network in Central Thailand. *Urban Water J* 275–282.
- Glezer, V., Harris, B., Tal, N., Iosefzon, B., Lev, O., 1999. Hydrolysis of Haloacetonitriles : linear Free Energy Relationship, Kinetics and Products. *Water Res* 33, 1938–1948.
- Guilherme, S., Rodriguez, M.J., 2017. Models for estimation of the presence of non-regulated disinfection by-products in small drinking water systems. *Environ. Monit. Assess.* 189 (11), 577.
- Heller-Grossman, L., Idin, A., Limoni-Relis, B., Rebhun, M., 1999. Formation of cyanogen bromide and other volatile DBPs in the disinfection of bromide-rich lake water. *Environ. Sci. Technol.* 33 (6), 932–937.
- Hua, G., Reckhow, D.A., Kim, J., 2006. Effect of Bromide and Iodide Ions on the Formation and Speciation of DBPs during Chlorination. *Environ. Sci. Technol.* 40 (9), 3050–3056.
- Huo, S., Xi, B., Yu, H., Qin, Y., Zan, F., Zhang, J., 2013. Characteristics and transformations of dissolved organic nitrogen in municipal biological nitrogen removal wastewater treatment plants. *Environ. Res. Lett.* 8.
- Ike, I.A., Karanfil, T., Ray, S.K., Hur, J., 2020. A comprehensive review of mathematical models developed for the estimation of organic disinfection byproducts. *Chemosphere* 246, 125797.
- Kanan, A., Karanfil, T., 2020. Estimation of haloacetonitriles formation in water: uniform formation conditions versus formation potential tests. *Sci. Total Environ.* 744, 140987.
- Krasner, S.W., McGuire, M., Jacangelo, J.G., Patania, N.L., Reagan, K., Aieta, E.M., 1989a. The Occurrence of Disinfection By-products in US Drinking Water. *J Am Water Works Assoc* 81 (8), 41–53.
- Krasner, S.W., Weinberg, H.S., Richardson, S.D., Pastor, S.J., Chinn, R., Scimenti, M.J., Onstad, G.D., Thruston, A.D., 2006. Occurrence of a new generation of disinfection byproducts. *Environ. Sci. Technol.* 40, 7175–7185.
- Krasner, S.W., Westerhoff, P.K., Chen, B., Amy, G., Nam, S.-N., Chowdhury, Z.K., Sinha, S., Rittmann, B.E., 2008. Research Report: Contribution of Wastewater to DBP Formation. American Water Works Association.
- Krasner, S.W., McGuire, M.J., Jacangelo, J.G., Patania, N.L., Reagan, K.M., Aieta, E.M., 1989b. The occurrence of disinfection by-products in US drinking water. *J. Am. Water Works Assoc.* 81, 41–53.
- Kolla, R.B., 2004. Formation and Modeling of Disinfect Ion By-Products in Newfoundland communities. Memorial University of Newfoundland, NL, Canada. Masters Thesis.
- Lee, W., Westerhoff, P., Croué, J.-P., 2007. Dissolved Organic Nitrogen as a Precursor for Chloroform. *Trichloronitromethane SUVA* 41, 5485–5490.
- Lee, W., Westerhoff, P., 2009. Formation of organic chloramines during water disinfection – chlorination versus chloramination. *Water Res* 43, 2233–2239.
- Lin, J., Chen, X., Zhu, A., Hong, H., Liang, Y., Suna, H., Lin, H., Chen, J., 2018. Regression models evaluating THMs, HAAs and HANs formation upon chloramination of source water collected from Yangtze River Delta Region. China. *Ecotoxicol. Environ. Saf.* 160, 249–256.
- Liu, C., Ersan, M.S., Plewa, M.J., Amy, G., Karanfil, T., 2018. Formation of regulated and unregulated disinfection byproducts during chlorination of algal organic matter extracted from freshwater and marine algae. *Water Res* 142, 313–324.
- Liu, C., Ersan, M.S., Plewa, M.J., Amy, G., Karan, T., 2019. Formation of iodinated trihalomethanes and noniodinated disinfection byproducts during chloramination of algal organic matter extracted from *Microcystis aeruginosa*. *Water Res* 162, 115–126.

- Mian, H.R., Chhipi-Shrestha, G., Hewage, K., Rodriguez, M.J., Sadi, R., 2020. Predicting unregulated disinfection by-products in small water distribution networks: an empirical modelling framework. *Environ. Monit. Assess.* 192, 497.
- Milot, J., Rodriguez, M.J., Serodes, J.B., 2002. Contribution of neural networks for modeling trihalomethanes occurrence in drinking water. *J. Water Resour. Plan. Manag.* 128, 370–376.
- Morrow, C.M., Minear, R.A., 1987. Use of Regression Models to Link Raw Water Characteristics to Trihalomethane Concentrations in Drinking Water. *Water Res.* 21, 41–48.
- Muellner, M.G., Wagner, E.D., McCalla, K., Richardson, S.D., Woo, Y.T., Plewa, M.J., 2007. Haloacetonitriles vs. regulated haloacetic acids: are nitrogen containing DBPs more toxic? *Environ. Sci. Technol.* 41 (2), 645–651.
- Na, C.Z., Olson, T.M., 2004. Stability of cyanogen chloride in the presence of free chlorine and monochloramine. *Environ. Sci. Technol.* 38 (22), 6037–6043.
- Nikolaou, A.D., Lekkas, T.D., Golfinopoulos, S.K., 2004. Kinetics of the formation and decomposition of chlorination by-products in surface waters. *Chem. Eng. J.* 100, 139–148.
- Obolensky, A., Singer, P.C., Asce, M., Shukairy, H.M., 2007. Information collection rule data evaluation and analysis to support impacts on disinfection by-product formation. *J. Environ. Eng.* 133, 53–63.
- Oliver, B.G., 1983. Dihaloacetonitriles in drinking-water - algae and fulvic-acid as precursors. *Environ. Sci. Technol.* 17, 80–83.
- Platikanov, S., Martin, J., Tauler, R., 2012. Linear and non-linear chemometric modeling of THM formation in Barcelona's water treatment plant. *Sci. Total Environ.* 432, 365–374.
- Plewa, M.J., Wagner, E.D., Muellner, M.G., Hsu, K.M., Richardson, S.D., 2008. Comparative mammalian cell toxicity of N-DBPs and C-DBPs. Chapter 3. In: Karanfil, T., Krasner, S.W., Westerhoff, P., Xie, Y. (Eds.), Occurrence, Formation, Health Effects and Control of Disinfection By-Products in Drinking Water. American Chemical Society, Washington, DC, pp. 36–50.
- Reckhow, D.A., Malcolm, R.L., Survey, U.S.G., 1990. Chlorination of humic materials: byproduct formation and chemical interpretations 24, 1655–1664.
- Reckhow, D.A., Platt, T.L., Macneill, A.L., McClellan, J.N., 2001. Formation and degradation of DCAN in drinking waters. *J. Water Supply Res. Technol.* 50 (1), 1–13.
- Roux, J.Le, Croue, J., 2012. Formation of NDMA and Halogenated DBPs by chloramination of tertiary amines: the influence of bromide ion. *Environ. Sci. Technol.* 46 (3), 1581–1589.
- Rook, J.J., 1974. Formation of haloforms during chlorination of natural water. *Water Treat. Examination.* 23, 234–243.
- Sfynia, C., Bond, T., Ganidi, N., Kanda, R., Templeton, M.R., 2017. Predicting the formation of haloacetonitriles and haloacetamides by simulated distribution system tests. *Procedia Eng.* 186, 186–192.
- Singer, P.C., Obolensky, A., Greiner, A., 1995. Trihalomethane formation in North Carolina drinking waters. *J. AWWA* 83–92.
- Sohn, J., Amy, G., Cho, J., Lee, Y., Yoon, Y., 2004. Disinfectant decay and disinfection by-products formation model development : chlorination and ozonation by-products. *Water Res.* 38, 2461–2478.
- Soyluoglu, M., Ersan, M.S., Ateia, M., Karan, T., 2020. Removal of bromide from natural waters : bromide-selective vs . conventional ion exchange resins. *Chemosphere* 238, 124583.
- Summers, R.S., Hooper, S.M., Shukairy, H.M., Solarik, G., Owen, D., 1996. Assessing DBP yield: uniform formation conditions. *J. Am. Water Works Assoc.* 88, 80–93.
- Trehy, M.L., Bieber, T.I., 1981. Detection, identification, and quantitative analysis of dihaloacetonitriles in chlorinated natural waters. In: Keith, L.H. (Ed.), Advances in the Identification and Analysis of Organic Pollutants in Water. Ann Arbor Science, Ann Arbor, MI, pp. 941–975.
- Uyak, V., Toroz, I., Meri, S., 2005. Monitoring and modeling of trihalomethanes (THMs) for a water treatment plant in Istanbul. *Desalination* 176, 91–101.
- Westerhoff, P., Debroux, J., Amy, G.L., Gatel, D., Mary, V., Cavard, J., 2000. Applying DBP models to full-scale plants. *J. AWWA* 89–102.
- Xue, C., Wang, Q., Chu, W., Templeton, M.R., 2014. Chemosphere The impact of changes in source water quality on trihalomethane and haloacetonitrile formation in chlorinated drinking water. *Chemosphere* 117, 251–255.
- Yang, X., Shang, C., Lee, W., Westerhoff, P., Fan, C., 2008. Correlations between organic matter properties and DBP formation during chloramination. *Water Res.* 42, 2329–2339.
- Yang, X., Shang, C., Westerhoff, P., 2007. Factors affecting formation of haloacetonitriles, haloketones, chloropicrin and cyanogen halides during chloramination. *Water Res.* 41, 1193–1200.
- Yu, Y., Reckhow, D.A., 2015. Kinetic analysis of haloacetonitrile stability in drinking waters. *Environ. Sci. Technol.* 49 (18), 11028–11036.
- Zhang, X., Yang, H., Wang, X., Fu, J., Xie, Y.F., 2013. Chemosphere Formation of disinfection by-products : effect of temperature and kinetic modeling. *Chemosphere* 90, 634–639.